NANOSCALE CHLORINE ISOTOPE HETEROGENEITY IN MARTIAN APATITE. J. R. Darling[1], L. F. White[2], T. Kizovski[2]., A. Černok[2], K. T. Tait[2], D. E. Moser[3], J. Dunlop[1], B. Langelier[4], J. O. Douglas[5], X. Zhao[6], I. Franchi[6] & M. Anand[6], [1]School of the Environment, Geography and Geosciences, University of Portsmouth, james.darling@port.ac.uk, [2]Centre for Applied Planetary Mineralogy, Royal Ontario Museum, [3]ZAPLab, University of Western Ontario, [4]Canadian Centre for Electron Microscopy, McMaster University, [5]Department of Materials, University of Oxford, [6]Planetary and Space Sciences, The Open University.

Introduction: Apatite group minerals offer a window into the volatile inventory of planetary bodies. They are widespread in martian meteorites, and are thought to have crystallized in the late stages of magma evolution [1, 2]. This has led to extensive efforts to characterize their halogen and OH content, D/H ratios and chlorine isotopic ratios [3–8]. Chlorine does not exhibit appreciable isotopic fractionation at high temperatures [4, 8], and can therefore provide insights into the composition of the martian lithosphere and interaction of magmas with surface reservoirs.

Within the shergottites, halogen contents and chlorine isotope ratios in chlorapatite are much more wide-ranging than in igneous rocks from Earth. They have up to ~6.6 ‰ variation in δ^{37}Cl, which is hypothesized to reflect mixing between mantle (-4 to -6 ‰) and crustal reservoirs [4, 6–8]. However, both isotopically heavy and light surface reservoirs have been proposed [6] and there is also evidence for intra-grain volatile element heterogeneity linked to impact melting [9]. The full range of causes of this variability and the influence on chlorine isotope systematics are not fully understood.

Most martian meteorites have clear evidence for intensive impact-generated deformation and metamorphism, yet little is known about how these shock-metamorphic processes manifest in apatite group minerals and influence their important chemical and isotopic records. Here we report on detailed nanostructural, chemical and chlorine-isotope analysis of chlorapatite in the highly-shocked shergottite Northwest Africa (NWA) 5298, including the first use of atom probe tomography (APT) for chlorine-isotope measurements.

Materials and Methods: Analyses were performed on a thin-section of NWA 5298, accession M53387 of the Royal Ontario Museum. Petrological evidence for shock metamorphism includes vesicular plagioclase melt, maskelynite, pockets of impact melt, and partial granularization of clinopyroxene, all formed in a single shock event that overprints a simple igneous texture [10–12].

Scanning electron microscopy (SEM), including electron backscatter diffraction (EBSD) was undertaken at the University of Portsmouth, UK. Further nanostructural and chemical measurements of targeted chlorapatite were undertaken by (scanning) transmission electron microscopy (STEM, University of Warwick, UK).

The CAMECA NanoSIMS 50L secondary ion mass spectrometer at the Open University was used to measure Cl abundances and isotopic ratios, following the methods of [13]. Nanoscale chemical and isotopic variability was further investigated by atom probe tomography (APT), using a CAMECA LEAP 5000 XR at the University of Oxford, UK, and CAMECA LEAP 4000 XR at McMaster University, Canada. δ^{37}Cl were determined from APT mass spectra using background-corrected peaks at 35 and 37 Da.

Chlorapatite nanostructures: Despite most apatites appearing smooth and relatively featureless in backscattered electron (BSE) imaging, all of the grains studied by EBSD have a complex internal structure (Fig. 1). We have identified different chlorapatite domains with evidence for planar deformation features, melting and recrystallization, annealing, high-densities of subgrain boundaries and low-densities of subgrain boundaries within the single studied thin-section. The latter domains are interpreted to represent preserved primary apatite that has not undergone major structural modification. APT and STEM energy dispersive X-ray spectroscopy (STEM-EDS) analysis demonstrate that Fe and some trace elements (Si and Pb), are enriched in nanoscale boundaries (Fig. 2). Additional evidence for mobility of minor and trace elements is provided by

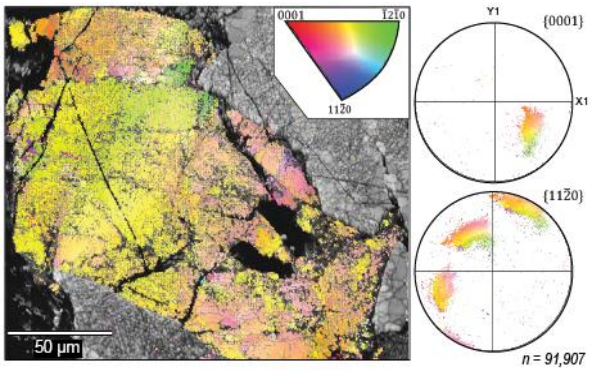

Figure 1: *EBSD data showing highly-deformed nature of NWA 5298 chlorapatite, with tens of degrees of misorientation, networks of low-angle (<10°) boundaries and some granularization. Map shows inverse pole figure coloring of crystallographic orientation.*

nanoclustering of Fe, Mn and Ti atoms.

Chlorine Isotope Results: A total of six NanoSIMS measurements were made on chlorapatites in NWA 5298, targeting the different nanostructural states identified by EBSD and Raman spectroscopy. These yielded a range of $\delta^{37}Cl_{SMOC}$ values (-3 to +1 ‰) that is as large as the range of all previous measurements from basaltic shergottites. There is a clear relationship between nanostructures and measured $\delta^{37}Cl_{SMOC}$. The single positive measured ratio (1.08 ± 0.75 ‰) comes from a domain with evidence for melting and recrystallization. The most negative values (around -3 ‰) were measured in domains with a high-density of subgrain boundaries. Intermediate values were measured from the least nanostructurally complex grain, apatite 3, in areas with lower densities of subgrain boundaries.

Chlorine concentration and isotope ratio data were also derived from APT datasets. The values from individual nanoscale tips (<0.001 μm^3) range from -12.5 ± 4.8 ‰ to 3.7 ± 5.3 ‰ (2σ), and the concatenated dataset (all APT tips linked into one mass spectra) has a $\delta^{37}Cl_{SMOC}$ value of -1.7 ± 2.2 ‰, which is within uncertainty of the NanoSIMS results from the same grain. Isolated nanoscale boundaries have highly-negative $\delta^{37}Cl_{SMOC}$ values (-12.0 ± 4.2 to -45.3 ± 17.8 ‰), albeit with large uncertainties due to the limited ion counts, and elevated Cl contents compared to microscale measurements.

Findings: Chlorapatite grains in NWA 5298 have been highly deformed and variably recrystallized by the shock event that has affected this rock (>30 GPa; [12]). Notably, shock nanostructures link with chemical heterogeneities and Cl isotope variations at micro to nano-scales. We present a new approach to studying Cl isotope systematics from sub-micron volumes of chlorapatite using atom probe tomography, demonstrating that accurate Cl isotope ratios can be measured at precision of ~ 2 ‰ using this approach. Our results resolve significant nanoscale chlorine isotope heterogeneity in NWA 5298, which we interpret to result from mobilization of isotopically light chlorine along nanoscale boundaries during the shock event responsible for launch.

This combined EBSD, NanoSIMS and atom probe tomography (APT) approach has tremendous potential to resolve primary and secondary isotopic compositions of challenging planetary samples, such as returned samples from the Moon, Mars, and the asteroid belt. In this case, the best estimate of the primary chlorine isotopic composition of NWA 5298 is provided by NanoSIMS measurements of the least nanostructurally complex subgrain domains.

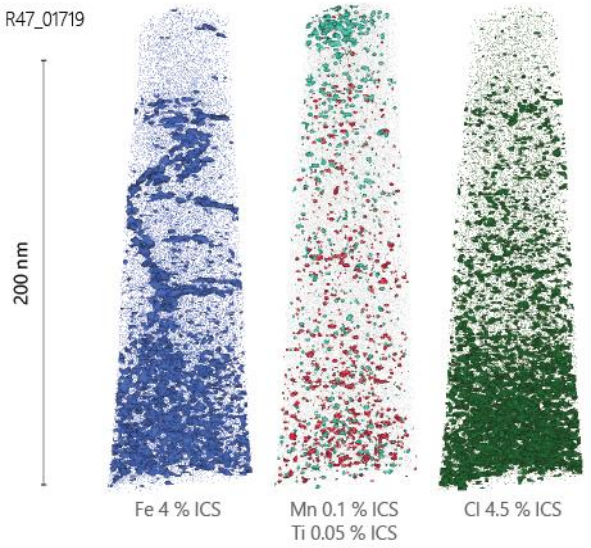

Figure 2: *Atom probe tomography data highlighting Fe-enriched nanoscale boundaries (left), clustering of Mn and Ti (center) and variations in Cl content defined by isoconcentration surfaces (ICS).*

Acknowledgments: This work was funded by Royal Society grant RG160237 and STFC grants ST/S000291/1 to JD and ST/P000657/1 to MA and IAF, along with UoP support for FIB-SEM and STEM access. We thank Geoff Long for sample preparation wizardry at UoP and Geoff West for assistance with FIB-SEM and STEM analysis at Warwick. The LEAP 5000XR at the Department of Materials, Oxford was funded by EPSRC (EP/M022803/1)

References: [1] Filiberto J. and Treiman A. H. (2009) *Geology 37*, 1087–1090. [2] McCubbin F. M. et al. (2012) *Geology* 683–687. [3] Hallis L. J. et al. (2012) *Earth & Planet. Sci. Lett. 359–360*, 84–92. [4] Williams J. T. et al. (2016) *Meteoritics & Planet. Sci. 51*, 2092–2110. [5] Weis F. A. et al. (2017) *GCA 212*, 84–98. [6] Bellucci J. J. et al. (2017) *Earth & Planet. Sci. Lett. 458*, 192–202. [7] Shearer C. K. et al. (2018) *GCA 234*, 24–36. [8] Sharp et al., (2016) *Meteoritics & Planet. Sci. 51*, 2111–2126. [9] Howarth G. H. et al. (2015) *GCA 166*, 234–248. [10] Irving A. J. et al. (2008) *Meteoritics & Planet. Sci.* 43, 5332. [11] Hui H. et al. (2011) *Meteoritics & Planet. Sci. 46*, 1313-1328. [12] Darling J. R. et al. (2016) *Earth & Planet. Sci. Lett. 444*, 1–12. [13] Barnes J. J. et al. (2016) *Earth & Planet. Sci. Lett. 447*, 84–94.